

On the State-of-the-Art of Real-Time GNSS Signal Acquisition – a Comparison of Time and Frequency Domain Methods

Thomas Pany*, E. Göhler*, M. Irsigler* and J. Winkel*

*IFEN GmbH, Poing, Germany. Email: t.pany@ifen.com

Abstract—This paper summarizes what is needed to achieve a real-time -157 dBm GPS C/A signal acquisition sensitivity in ASIC and software receiver implementations for a cold and a warm start. Two receivers (one ASIC receiver working in the time domain and one PC software receiver working in the frequency domain) are implemented in a highly efficient way. The algorithms are outlined here and are tested with a GNSS signal simulator. Both use the same RF front end, operate on identical 2-bit samples and produce identical correlation results. The sensitivity comparison is completed by including some new commercial GPS chip evaluation boards in the test runs. We demonstrate the importance of narrow band and strong signal interference mitigation and investigate the role of the coherent integration time length as an important trade-off parameter.

Keywords—GPS, acquisition, FFT, ASIC, software receiver, time domain correlation, frequency domain correlation

I. INTRODUCTION

High sensitivity GNSS signal acquisition is a technique that is more than ten years old and has revolutionized the GPS receiver market by extending the GPS service availability and allowing integration of GPS chips into mobile phone handsets using cheap and low performing antennas.

For the purpose of this paper, we understand acquisition to be the process to estimate the code phase and Doppler values of GNSS signals from the intermediate frequency (IF) samples that are accurate enough to start tracking. This is achieved by correlating the samples with replica signals whose parameters are taken from a two-dimensional grid of code phase and Doppler values. As the sensitivity increases, interference effects become more pronounced and must be accounted for as shown in Fig. 1.

For a sufficiently short time interval, the received signal's carrier phase increases linearly in time (= constant Doppler).

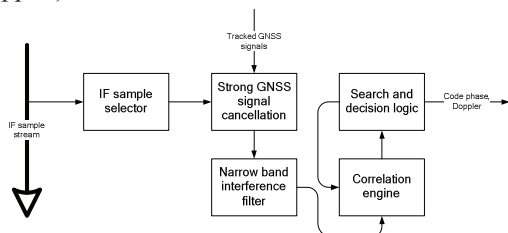


Figure 1. High sensitivity GNSS signal acquisition

If we further assume a constant amplitude and a uniformly distributed initial carrier phase, the generalized maximum likelihood ratio detector of [8]

$$\hat{\tau}, \hat{\omega} = \arg \max_{\tau, \omega} \left| \int_{t=0}^{T_{coh}} s(t) c(t-\tau) \exp(-2\pi i \omega t) dt \right|^2 \quad (1)$$

decides that the signal is present, if the correlation value of (1) evaluated with the estimated parameters exceeds a threshold. Here s is the received signal, c is a PRN code replica including the modulation scheme, ω is the angular Doppler, τ is the code phase and T_{coh} is the coherent integration time. A ‘hat’ symbol denotes estimated parameters. The generalized likelihood ratio detector is not optimal in a theoretical sense (i.e. there is no mathematical proof that it maximizes the detection probability for a limited false alarm rate) but to our best knowledge no better detector has been proposed in the context of non-random parameter estimation [8, 10]. If prior information on the code phase and Doppler distribution is provided, Bayesian techniques are a possible way forward [4]. The coherent integration (1) can be realized with time domain and frequency domain techniques.

A. Time Domain Correlation

Reasonable acquisition in time domain requires a large number of correlators to detect signals quickly. One way of doing that is the explicit convolution computation as a discrete sum according to (1) while trying several Doppler bins separately:

$$S_k = \int_{t_k}^{t_k + T_{chip}} s(t) \exp(2\pi i \omega_k t) dt \quad (2)$$

$$\hat{\tau}(j), \hat{\omega} = \arg \max_{j, \omega} \left| \sum_{k=1}^N S_k \exp(-2\pi i \omega_k) c_{j-k} \right|^2$$

For a periodic replica of length N a less extensive approach is to use a matched filter that feeds in the samples (or small sums of baseband samples S_k over the duration of one chip) and compute the correlation value each time by multiplying all input values with the replica and summing up the result. For that the input values S_k are fed into a register bank F_m , and for each new input value S_{k+1} the registers are shifted:

$$\begin{aligned}
k &\rightarrow k+1: \\
F_1^{(k+1)} &= S_k \\
F_n^{(k+1)} &= F_{n-1}^{(k)} \\
Corr_k(\omega) &= \left| \sum_{n=1}^N F_n^{(k)} \exp(-2\pi i \omega t_n) c_n \right|^2 \\
\hat{\tau}(k), \hat{\omega} &= \arg \max_{k, \omega} Corr_k(\omega)
\end{aligned} \tag{3}$$

Doppler removal may be performed either by equipping a complex replica with a negative rotation with the Doppler frequency, or by mixing the input samples into the base band in advance (by associating the exponential factor in (2) either with the input values S_k or replica chips c_k).

The advantage of this approach is its simplicity and easy adaption as a hardware algorithm. It may also easily be expressed in integer arithmetic; quantization noise is small even for very small bit sizes. The other advantage is the streaming nature of it because for each input value an output value is immediately computed. This meets the typical pipeline form of hardware architecture that passes the values for various processing stages each clock time and allows the building of complex algorithms without specific timing problems. If correlation values are kept in memory they may be scanned for as described in subsection I.D.

B. Frequency Domain Correlation

Spread spectrum code acquisition with Fourier techniques was first described in 1990 by Cheng et al. to search one Doppler bin for all code phase values in parallel by employing the convolutional theorem [3]. Using the notation of [10], the coherent integration is the product of the two discrete Fourier transforms of the sampled received signal and the code replica:

$$\hat{\tau}(k), \hat{\omega}(p) = \arg \max_{k, p} \left| \text{IFFT} \left\{ \text{FLIP} \left\{ \text{FFT} \{c\} \text{SHIFT}_p \left\{ \text{FFT} \{s\} \right\} \right\} \right\} \right|^2 \tag{4}$$

The code replica transform is flipped (the last index goes to the first place) and the received signal transform is periodically shifted by p elements depending on the considered Doppler shift. The index k of the inverse transform corresponds to the code phase shift.

For quasi periodic PRN code signals like the C/A code (it repeats itself 20 times within one data bit), the coherent integration time can be extended from one to multiple milliseconds with Doppler preprocessing causing only small additional computational costs as pointed out by Akopian et al. some years ago [1]. For tiered code signals, a Doppler preprocessing method focusing on peaks of the secondary code spectrum uses a similar methodology but needs generally a higher computational load [10]. This method will be used in section III. If precise time assistance data is available, the inverse FFT of the convolutional theorem can be expressed with a much smaller length, thereby reducing the computational load [14].

C. Interference

GNSS signal acquisition is typically degraded by two prominent interference sources: strong GNSS signals and narrowband interference. The cross correlation protection of GNSS signals is typically smaller than signal power variations in an indoor environment. Therefore cross correlation peaks of the considered PRN code with the received signal's contributions from other strong satellites will be higher than the correlation peak of the considered PRN code with the matching satellite signal. Several methods exist to cope with this interference. Ad hoc methods exclude Doppler bins, which are more affected by cross correlation peaks, and search only unaffected regions [9]. Signal cancellation techniques retrieve the strong signal's code phase, Doppler, carrier phase and amplitude values from the tracking channel, reconstruct a replica signal and subtract it from the received signal prior to correlation as shown in Fig. 1. This method will be used in section III. A rigorous way is to simultaneously estimate the vector of code phases τ and Doppler values ω for all M signals with a formula like [5].

$$\hat{\tau}, \hat{\omega} = \arg \max_{\tau, \omega} R_{c,s} R_{c,c}^{-1} R_{c,s}^* \tag{5}$$

Here $R_{c,s}$ denotes a vector of length M with the complex valued correlations of the received signal with the M replica signals. $R_{c,c}$ is a correlation matrix of size $M \times M$ of the replica signals with themselves. Both matrices depend on the M code phase values τ and M Doppler values ω .

Narrowband interference occurs often due to coupling of unwanted digital frequencies into the analog domain. The effect of narrowband interference can be understood if the received signal $s(t)$ in (1) is replaced by a sinusoidal term. It merges with the exponential of (1) and the correlation result is the corresponding Fourier component of the PRN code. As a characteristic, the correlation result is independent of the code phase. Narrowband interference can be mitigated with adaptive notch filters or short time FFT methods [16].

D. Detectors

The assumption of a strictly constant Doppler and a linear carrier phase holds only for short intervals due to data bit/symbol transitions, user/satellite motion or clock jitter. To further increase the total integration time, several coherent correlation results for the same Doppler and code phase (eventually accounting for the code Doppler) can be combined if the carrier phase dependency is removed via a magnitude squaring operation or by multiplying two timely consecutive correlation values (differential detector) [15]. The squaring operation derives from the Maximum Likelihood principle if we assume in all intervals a constant Doppler and an independent and uniformly distributed carrier phase at the start of each coherent integration interval [10]. The accumulated correlation results are compared against a threshold. Either the code phase and Doppler corresponding to the largest post-correlation SNR are used to initialize a tracking channel or the m -largest values are used in a second test using a supplementary correlator bank [2]. The threshold depends on the noise floor that can be measured with pre-correlation [10] or post-correlation methods [17]. In the latter case, the noise floor estimation handles the effect of interference better.

II. INTRACK HARDWARE ACQUISITION ASIC

As an example of a high sensitivity and time domain acquisition, the IFEN INTrack ASIC is used, which can be configured for a variety of GNSS signals.

A. Hardware Setup

The ASIC is the core of the IFEN INTrack system, which consists of three main components as shown in Figure 2 – a navigation process running on a COTS processor, the INTrack ASIC that runs the acquisition and tracking, and the RF front end that performs analogue filtering, amplification, down conversion and digitalization.

The INTrack ASIC implements a massive parallel correlation machine in the matched filter fashion with pre-correlation carrier wipe off. The acquisition runs in parallel on separate channels and has a double buffered correlation for coherent and noncoherent integration, and an elaborated mixed signal tracking mechanism in several channels [18]. This architecture (Figure 3) allows the running of either a larger set of Doppler bins in parallel for the same code, or the running of a scan over different PRN codes. The coherent integration time may be set from 1 to 200 ms and up to 2 s for noncoherent integration. Eventually a data wipe-off is used.

B. Coherent/Noncoherent Integration

The coherent integration into the first correlation RAM is a sum of the complex correlation values $Corr_k$ while the noncoherent result is a magnitude squared sum of the coherent integrated values. After the acquisition run has been completed, the ten topmost values are reported, and the resulting correlation values may be read sequentially. Data bit transitions on the coherent integration will degrade the correlation peak as shown in (11) and residual Doppler offsets have an impact according to (7). Especially some Doppler variations due to clock drift changes or user/SV motion will degrade the correlation value.

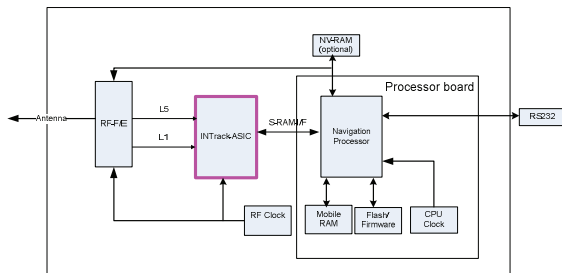


Figure 2. INTrack system

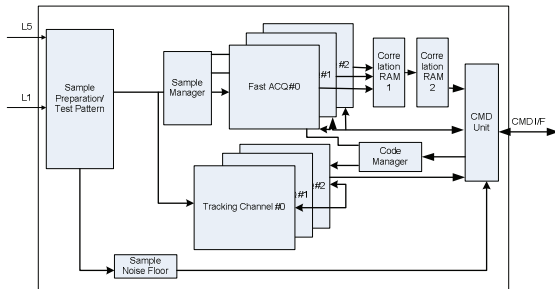


Figure 3. INTrack block diagram with a time domain acquisition scheme

TABLE I.
TIME DOMAIN ACQUISITION TIME FOR GPS C/A

Parameter	Estimate
Number of parallel acquisition channels	20
Single Doppler bin signal time	3.2 s
Doppler bin width	62.5 Hz
Number of Doppler bins per satellite	185
Single satellite search time	29.6 s
32 satellite search time	950 s
Effective number of correlators	20460

The design also has the flexibility to deliver partial coherent correlation products to a software post processing that may use an advanced coherent/noncoherent approach (e.g. differential detector [15]).

C. Detection

For signal detection, the same approaches may be used as for the frequency domain acquisition. Due to the sequential nature of the outcoming correlation values it is comparably easy to obtain the maximum values according to equation (1) in the hardware. The detection threshold either may be derived from a running pre-correlation noise estimation based on the input samples, or on the off-peak correlation values. The latter has the advantage that interfering signals that are out of the replica spectra envelope are ignored. For fast acquisition of nominal signals the investigation of the topmost correlation values may suffice.

D. Processing time

For the presented time domain scheme, the single Doppler bin acquisition time depends on the number of coherent (plus 1 to take into account the loading of the filter) and noncoherent integrations using a certain code epoch period (typically 1 msec for GPS C/A) plus a constant software read and processing time:

$$T_{acq} = (N_{coh} + 1)N_{non-coh}T_{code} + T_{read} \quad (6)$$

The limiting factors are the available hardware resources, especially the number of acquisition channels when searching several Doppler bins or satellites in parallel. Assuming for all satellites a 16 ms coherent integration time and 200 noncoherent integrations (as a baseline configuration for this paper) gives the result of Tab I.

Assisted information is easily integrated by the sequential processing of the input samples. For example, a data wipe-off may be easily performed on a dedicated FIFO whose entries are multiplied with the input samples once the acquisition is started at a certain time (as is the case for the INTrack ASIC implementation).

III. SOFTWARE RECEIVER ACQUISITION

For the IFEN SX Navigation Software Receiver [6] an efficient implementation of the Doppler preprocessing method has been selected based on the description in section 9.5.6 and 9.5.7 of [10]. It uses a combination of coherent and noncoherent integrations.

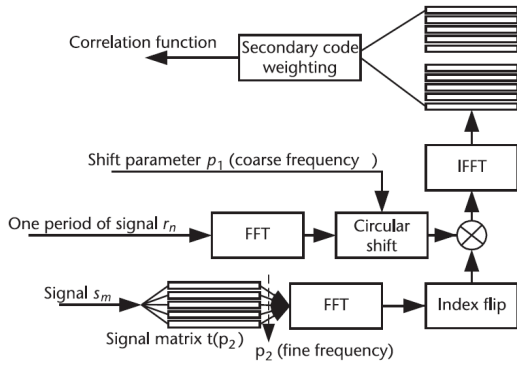


Figure 4. One coherent integration in the frequency domain with Doppler preprocessing and secondary code weighting

A. Coherent Integration

The coherent integration scheme is depicted in Figure 4. The batch of IF signal samples s_n corresponding to one coherent integration (e.g. 16 ms) is sub-divided in smaller mini-batches of the length of one primary PRN code (e.g. 1 ms for GPS C/A, 4 ms for Galileo E1). Those mini-batches are added yielding the signal matrix $t(p_2)$. Each row in this matrix is of the length of the primary PRN code and is the coherent summation of IF signal samples accounting for a fine Doppler frequency p_2 . The rows of the matrix undergo a one-dimensional FFT. Depending on the searched Doppler bin, the transformed rows are multiplied with the FFT of the primary PRN code r_n and an inverse FFT is done. Several inverse FFT results are combined to obtain the coherent integration result over the full period (e.g. 16 ms), which is identical to (4) but computationally much more efficient due to the use of shorter FFT lengths. If a trivial secondary code (all values = 1) is used, the secondary code weighting scheme is highly efficient and the searched Doppler bin number p receives contributions only from one coarse Doppler bin p_1 and one fine Doppler bin p_2 . Thus only one inverse FFT gives the desired correlation function [1].

B. Noncoherent Integration and Data Bit Transitions

Further noncoherent integrations are obtained by summing squared coherent correlation values. The batches are adjacent to each other, ignoring the presence of data bit transitions. A data bit transition during the coherent integration time reduces the correlation peak and causes a bias in the Doppler frequency estimation. With many noncoherent integrations, those losses become tolerable and the bias vanishes. Assuming that the code phase of the received signal and the replica signal match, the coherent correlation result can be written in the case of no data bit transition as:

$$P_{nobit}(\Delta\omega) = \left| \frac{1}{T_{coh}} \int_{t=0}^{T_{coh}} \exp\{-i\Delta\omega t\} dt \right|^2 \quad (7)$$

$$= \text{sinc}^2\left(\frac{\Delta\omega T_{coh}}{2}\right)$$

Here $\Delta\omega$ is the angular Doppler frequency error and P_{nobit} is the correlation result, which assumes 1 (=0 dB) in the ideal case. For the considered FFT method, the angular Doppler error is within $\Delta\omega \in [-\pi/T_{coh}, \pi/T_{coh}]$ and the maximum loss is $4/\pi^2 = -3.9$ dB. On average the Doppler loss is the expected value given by:

$$P_{nobit} = \langle P_{nobit}(\Delta\omega) \rangle_{\Delta\omega \in [-\frac{\pi}{T_{coh}}, \frac{\pi}{T_{coh}}]} = \frac{2(\pi \text{Si}(\pi) - 4)}{\pi^2} \quad (8)$$

The sine integral function is denoted as Si. This expression evaluates to -1.11 dB and is independent of the considered coherent integration time. In case a data bit transition is present, the calculation has to be extended and gives for a particular data bit transition time t_{bit} :

$$P_{bit}(\Delta\omega, t_{bit}) = \left| \frac{1}{T_{coh}} \left(\int_{t=0}^{t_{bit}} \exp\{i\Delta\omega t\} dt - \int_{t=t_{bit}}^{T_{coh}} \exp\{-i\Delta\omega t\} dt \right) \right|^2 \quad (9)$$

On average the expected value is:

$$P_{bit} = \langle P_{bit}(\Delta\omega) \rangle_{\substack{\Delta\omega \in [-\frac{\pi}{T_{coh}}, \frac{\pi}{T_{coh}}] \\ t_{bit} \in [0, T_{coh}]}} = \frac{2(\pi \text{Si}(\pi) - 4)}{\pi^2} \quad (10)$$

It evaluates to -4.34 dB. For a long total integration interval, only a fraction of the coherent integrations will be degraded by data bit transitions. The fraction is given by the ratio of the coherent integration time divided by two times the data bit/symbol length T_{bit} . For $T_{coh} \leq T_{bit}$, the combined Doppler/data bit loss is:

$$P = \frac{T_{coh}}{2T_{bit}} P_{bit} + \left(1 - \frac{T_{coh}}{2T_{bit}}\right) P_{nobit} \quad (11)$$

For a data bit length of 20 ms and a coherent integration time of 16 ms, this evaluates to -2.14 dB. This value is only ~ 1 dB worse compared to the case of no data bit transition. A situation with no data bit transitions can be achieved for pilot signals, for a data wipe-off or if the batches are subdivide in two mutually exclusive sets, where one is free of transitions (half-bit method, see e.g. [12]). Choosing a longer coherent integration time reduces the squaring loss but gives higher data bit losses. This must be traded off.

C. Verification and Interference

The frequency domain acquisition routine is tested with a real GPS C/A code signal. It was collected with a low noise figure active antenna inside our office building using a sample rate of 16.6 MHz and a bandwidth of 4 MHz. For acquisition, the signal is filtered and resampled to 4.096 MHz. We concentrate now on the acquisition of an attenuated signal of 20 dBHz from PRN10. The acquisition parameters are listed in Tab. II. The two strongest signals (directly received through a window) have 50 and 52 dBHz. Furthermore, we see in the digitized signal a narrowband interferer. The interferer C/N0 value is 49 dBHz corresponding to a jammer-to-signal ratio (for PRN10) of 29 dB.

With erfc being the complementary error function, the detection probability p_d can be approximated for a large number ν of non-coherent integrations [10] and is plotted for different single bin false alarm p_{fa} values in Fig. 5. This formula avoids the use of the noncentral chi-squared distribution and is accurate to 1 dB, which is useful when e.g. your MATLAB version does not directly support it.

TABLE II.
FREQUENCY DOMAIN PARAMETERS FOR GPS C/A

Parameter	Value
Coherent integration time	16 ms
Non-coherent integrations	200
Code phase resolution	0.25 chip
Doppler resolution	62.5 Hz
Number of Doppler bins in cold start	185
Primary FFT length (= number of code phase bins)	4096
Non-coherent integrations	200

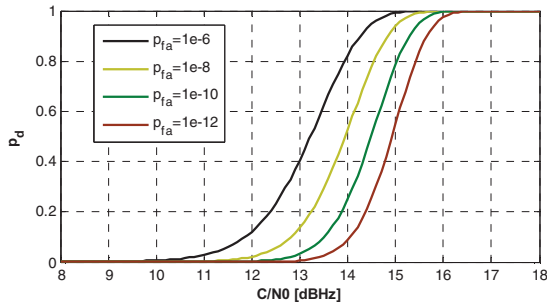


Figure 5. Detection probability p_d for different values of p_{fa} plotted as a function of C/N_0 , neglecting data bit transition and assuming perfect code phase and Doppler match for the values of Tab. II.

$$p_d = \frac{1}{2} \operatorname{erfc} \left(\frac{\operatorname{erfc}^{-1}(2p_{fa}) \sqrt{2v} - vT_{coh} C/N_0}{\sqrt{2v + 4vT_{coh} C/N_0}} \right). \quad (12)$$

With a Doppler span of ± 5780 Hz we need to search ~ 750000 bins (code phase plus Doppler dimension) per satellite. The system false detection probability is approximately the single bin false detection probability multiplied by the number of bins. Thus, if we want to achieve a system false detection probability (per satellite) of 1%, then the single bin probability is $\sim 10^{-8}$. In this case, the required C/N_0 is ~ 15 dBHz for $p_d = 90\%$. Adding the Doppler and data bit losses from above and neglecting the code phase mismatch losses, we would expect an average sensitivity of 17 dBHz.

An exemplary peak is depicted in Fig. 6. This peak is well above the noise floor but it is only visible if the narrow band interference and the strong GNSS signal cancellation are activated. If we deactivate the narrow band interference mitigation (done after the FFT), we get the result of Fig. 7. As expected, the interference correlates with the replica code and correlation lines for selected Doppler frequencies occur. The lines are separated 1 kHz corresponding to the PRN code length of 1 ms. The lines are broadened by 50 Hz, due to the presence of data bit transitions. Deactivating the strong signal cancellation algorithm results in Fig. 8. Cross-correlation peaks of the strong GPS signals with the PRN10 replica are much higher than the desired correlation peak. If either of the two interference mitigation mechanisms is deactivated (or both), a wrong acquisition result is obtained.

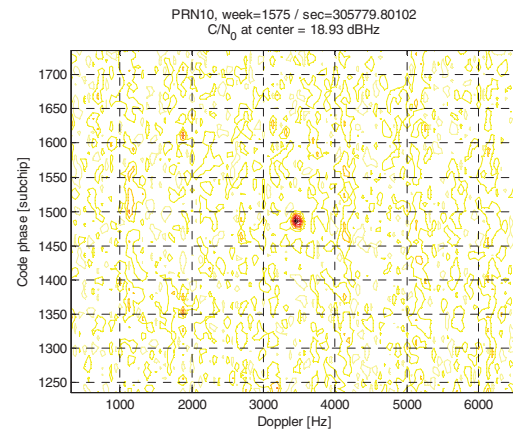


Figure 6. PRN10 (20 dBHz) acquisition result, narrow band and strong GPS signal interference mitigated

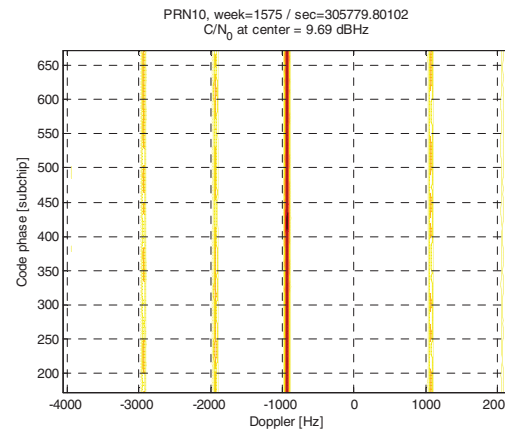


Figure 7. PRN10 (20 dBHz) acquisition result, strong GPS signal interference mitigated, narrow band interference retained

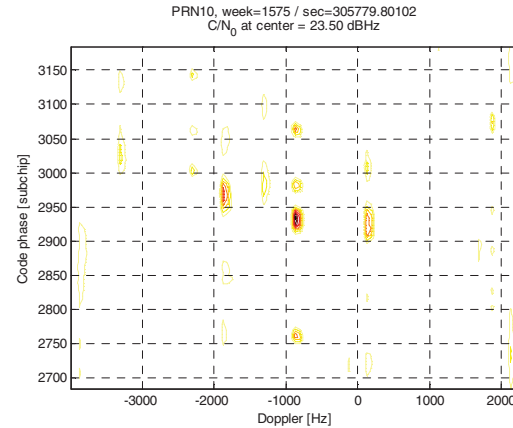


Figure 8. PRN10 (20 dBHz) acquisition result, strong GPS signal interference mitigated and narrow band interference retained

D. Computational Time

The algorithm has been implemented on an x86 platform and on a graphics processing unit (GPU) [13]. It is very well parallelizable, because the search of the different PRN codes or in different Doppler bins is largely independent of each other. We tested it on a PC equipped with two Intel Xeon 5472 CPUs, each having four cores and running with 3 GHz. Furthermore, the PC was equipped with an nVidia GTX 480 graphics card with 15

multiprocessors and 480 cores running at 1.4 GHz. This is high end equipment consuming more than a few hundred watts of electrical power.

A summary of the time needed to acquire all 32 GPS C/A PRN codes is shown in Tab. III. The data preparation includes the interference cancellation algorithm, resampling, subdivision into mini-batches and the forward FFT. Data preparation always runs on the CPU and takes around 1.1 – 1.6 s for a total signal time of 3.2. s. It also converts the 2-bit samples into a floating point representation. The maximum runtime of the algorithm is limited to be 10 s. A longer runtime would result in an unreliable code phase and Doppler extrapolation during the tracking handover. During this time the graphics card searches all PRN codes with 187 Doppler bins (two more than in Tab. II) in around 4 s. The CPU searches 16 PRN codes in around 10 s. The number of effective correlators is given by the number of bins (= product of number of PRNs, Doppler bins and code phase bins) multiplied by the total integration time and divided by the runtime of the algorithm. It is reasonable to compute this value with and without the data preparation time. Several millions of effective correlators can be obtained by a conventional PC especially if it is equipped with a graphics card.

IV. COMPARISONS

A. Conceptual Differences

Acquisition algorithms can not only be compared in terms of sensitivity. Most importantly, the number of mathematical operations or the number of gates defines the implementation costs. For a fixed Doppler search range, frequency domain techniques show an asymptotic $T_{coh}^a \cdot \log(T_{coh})$ increase of the required number of operations. The exponent a equals 2 for long PRN codes and 1 for short PRN codes [10]. Time domain correlation has an T_{coh}^3 increase. However, the matched filter structure is well implementable in an ASIC. The time domain correlation is also well suited for finite precision arithmetic using a low number of bits, whereas the frequency domain algorithm and the interference cancellation algorithms require a higher number of bits if not floating point arithmetic.

The time domain correlation works intrinsically in real-time and correlation results are available as soon as the last signal sample of an integration interval has been received. In fact the continuous increase of the correlation function can be monitored during several noncoherent integrations. Frequency domain techniques require buffering a number of samples before processing them.

TABLE III.
FREQUENCY DOMAIN ACQUISITION TIME

Parameter	GPU	CPU
Data preparation	1.125 s	1.593
Computed correlation values	24510464	12255232
Inverse FFT time	3.046 s	8.547 s
Signal Time	3.2 s	3.2 s
Eff. number of correlators (only IFFT)	25749667	4588363
Eff. number of correlators	18804480	3867529

Although this can be advantageous for the interference cancellation algorithms, it requires a large amount of memory and increases the latency. As a consequence, the estimated Doppler and code phase values have to be extrapolated to start tracking.

In the INTrack time domain correlation, code rate and Doppler shift can be freely adjusted. This allows for achieving a fine search grid size. Furthermore, the correlation can be performed synchronously with the PRN code, thereby avoiding data bit transitions during the coherent integration time, provided that the time is known better than the code period. Also a code Doppler can be compensated for perfectly. Frequency domain correlation allows only a finite Doppler bin size related to the coherent integration time causing the aforementioned Doppler and data bit losses. A code Doppler can be accounted for during the non-coherent integration, but every coherent integration has to be performed with the same replica signal and thus same code Doppler for computational simplicity. This can be problematic if very long coherent integration times are used.

Narrow band interference is easily mitigated in frequency domain simply by excising high spectral lines after the FFT. Time domain techniques may rely on adaptive notch filters.

B. Laboratory Tests

To gain further insight into the relation of frequency domain and time domain correlation, we connected the SX-NSR and the INTrack ASIC to the same GPS signal source (a NCS RF signal simulator). It generates the RF signal as it would be output by a GNSS antenna. Here, we focus on the acquisition of the GPS C/A code signal of PRN15. The frequency domain acquisition result is shown in Fig. 9. The algorithm estimates a C/N0 of 25.2 dBHz. When the signal is later tracked by the receiver, it estimates a C/N0 of 29.7 dBHz. Thus resampling, Doppler, code phase and data bit transition losses are 4.5 dB. In Fig. 10 the time domain result is plotted; the algorithm estimated a similar C/N0 of 25 dB Hz with limited accuracy of the acquisition peak estimation. In comparison with the frequency domain acquisition, a slight Doppler offset of 200 Hz is present due to the fact that the data was captured on different days using the same simulator setup but the real receiver oscillator frequency changes with time. But as expected, both receivers produce virtually the same two-dimensional correlation function in real time.

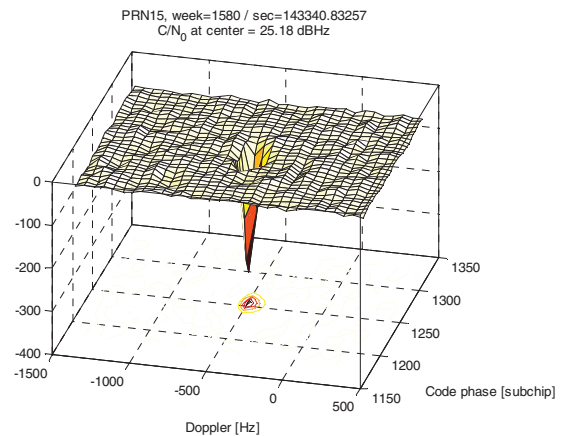


Figure 9. Frequency domain acquisition result (for better visualization the negative acquisition result is shown)

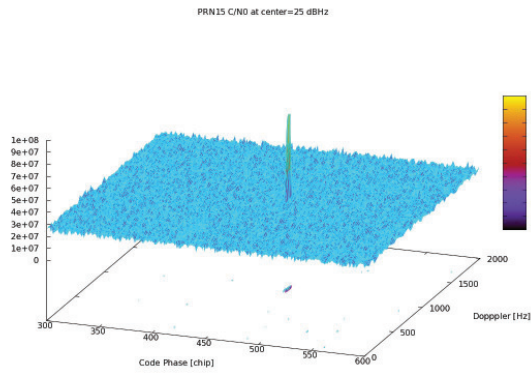


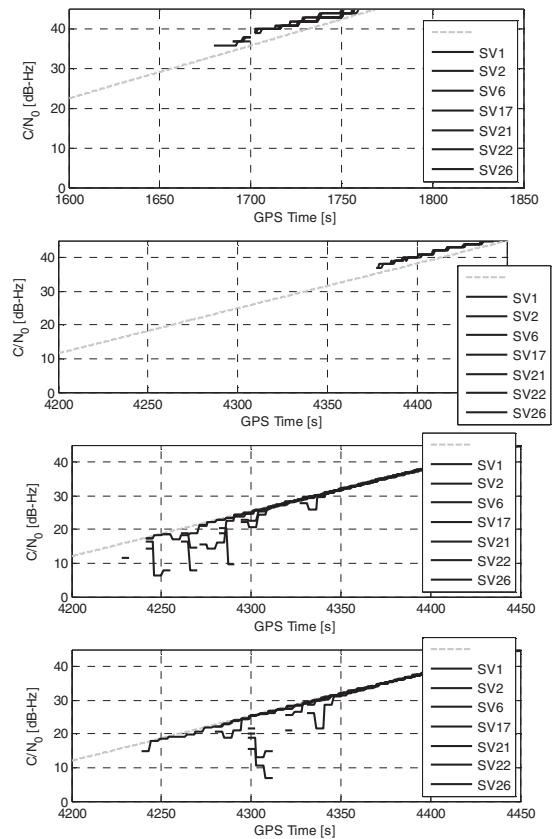
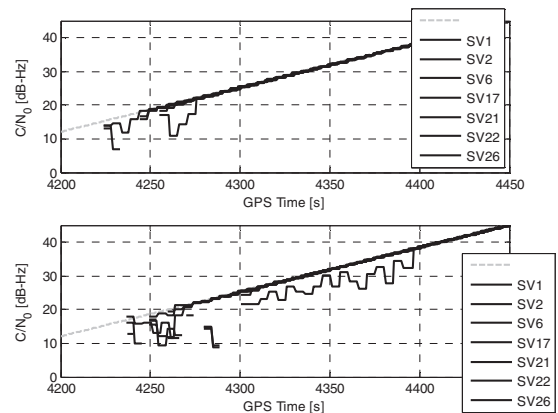
Figure 10. Time domain acquisition result

V. RAMP TESTS

This section tests the acquisition engine of the software receiver and two commercial chip sets using an RF signal generator in autonomous cold start in which the receiver has to search all PRN codes in the full Doppler range. We generate with the NCS RF signal generator a GPS C/A constellation signal, whose power increases linearly in time. At the beginning, the receiver is reset and we plot the estimated C/N_0 of the different PRNs once they are acquired and tracked. This test is similar to the one described in [7] but here we consider only results obtained in real time. This contrasts to dedicated post-processing methods, which are computationally even more demanding and achieve a higher sensitivity [11].

The C/N_0 time series is shown in Fig. 11. The first commercial ASIC mass market receiver acquires signals at around 35 dBHz but we suspect that it would acquire signals at lower C/N_0 if given more time. The second commercial mass market receivers start at around 37 dBHz. We may suspect that both receivers do not search all PRNs on all Doppler bins simultaneously, but also other steps like navigation message decoding may cause a delay until the receiver outputs C/N_0 values in the NMEA message. The frequency domain acquisition of the SX-NSR starts below 20 dBHz and the GPU module acquires the signal more quickly than the CPU module. The SX-NSR has sometimes difficulties to achieve bit-synchronization at very low C/N_0 and loses single signals again.

In a warm start scenario the SX-NSR is provided with assisted GPS data (ephemeris and clocks). In a mobile phone-assisted scenario we provide fine-time assistance (better than 1 ms) and the initial position accuracy is 15 km. In a continental wide assisted scenario, the timing accuracy is 0.5 s and the position accuracy is 5000 km. Assistance data helps to reduce the number of Doppler bins and the number of searched PRN codes. In the mobile phone assisted case, it helps the receiver to perform bit synchronization and in both cases it helps the receiver to perform frame synchronization. In the mobile phone assisted case, signals are already acquired at 15 dBHz. One signal requires 20 s to enter stable tracking. In the continental assisted case, tracking starts below 20 dBHz and one signal needs around 100 s to enter stable tracking. Signals, which are not in a stable tracking mode, are not considered for positioning.

Figure 11. Cold start ramp test: upper two: commercial mass-market ASICs, third: SX-NSR with GPU, lower (fourth): SX-NSR with CPU. The dashed line is the true C/N_0 value.Figure 12. SX-NSR GPU warm start sensitivity (upper: mobile phone assisted, lower: continental). The dashed line is the true C/N_0 value.

VI. CONCLUSIONS

In this work, a GPS C/A code acquisition based on 16 ms coherent integration with 200 noncoherent integrations has been investigated. This is a setting representative of the state-of-the-art in the year 2010. The coherent integration time is a compromise between squaring loss, data bit loss and Doppler estimation accuracy. This setting achieves a sensitivity of around 17 dBHz or -157 dBm, assuming a -174 dBm/Hz noise power density.

The time domain ASIC implementation can be configured to search 10 PRNs simultaneously in 2 Doppler bins, which is a warm start configuration. The PC software receiver frequency domain implementation may

use this configuration in an autonomous cold start searching all PRNs on all Doppler bins virtually simultaneously. This is important for professional and scientific applications, when no assistance data is available. Both implementations produce virtually identical correlation results and verify again that frequency and time domain acquisition engines can be exchanged. A proper handling of interference is essential to achieve this high sensitivity.

Finding optimal acquisition parameters for certain applications is a complex trade-off process involving much testing. Most likely, shorter coherent integration times shall be considered, as the number of Doppler bins is reduced and signals are acquired more quickly at the cost of a few decibels of increased squaring loss. Increasing the number of noncoherent integrations seems not the way to go, as the gain gradually diminishes. A further significant sensitivity increase can be expected, if a coherent integration time of several seconds is used. This is feasible at least in post-processing and allows acquisition of GPS C/A code signals at 0 dBHz [11].

Without fine time assistance, bit synchronization below or at the 20 dBHz level is one of the major difficulties after successful acquisition. It is required for stable DLL/FLL tracking, which needs 10 or 20 ms coherent integration and in contrast to acquisition does not tolerate bit transitions in the integration interval. They would cause large Doppler discriminator errors.

The presented methods can also be extended for other GNSS signals, but a possible secondary code, higher chipping rates and longer primary codes increase the computational demand.

ACKNOWLEDGMENT

This work has been partly performed within the DLR project INDOOR funded by the German Aerospace Center (DLR) on behalf of Federal Ministry of Economics and Technology (BMWi), IFEN Grant Contract No. FKZ 50 NA 0504.

REFERENCES

- [1] Akopian, D., "A Fast Satellite Acquisition Method," *Proc. ION-GPS 2001*, Salt Lake City, pp. 2871-2881, 2001.
- [2] Akopian, D., Sagiraju, P. K., and Turunen, S., "Performance of a two-stage massive correlator architecture for fast acquisition of GPS signals," *Proc. 2006 IEEE Region 5 Technical, Professional and Student Technical Conference*, San Antonio, 2006.
- [3] Cheng, U., Hurd, W. J., and Statman, J. I., Spread-Spectrum Code Acquisition in the Presence of Doppler Shift and Data Modulation *IEEE Trans. Commun.*, vol. 38, pp. 241-250, 1990.
- [4] Closas Gómez, P., Bayesian Signal Processing Techniques for GNSS Receivers: From Multipath Mitigation to Positioning 2009. Universitat Politecnica de Catalunya.North Campus, Jordi Girona 1-3, 08034 Barcelona.
- [5] Closas, P., Fernández-Prades, C., and Fernández-Rubio, J. A., Maximum Likelihood Estimation of Position in GNSS *IEEE Signal Processing Letters*, vol. 14, pp. 359-362, 2007.
- [6] Falk, N., Hartmann, T., Kern, H., Riedl, B., Pany, T., Wolf, R., and Winkel, J., "SX-NSR 2.0 - A Multi-frequency and Multi-sensor Software Receiver with a Quad-band RF Front End," *Proc. ION-GNSS 2010*, Portland, pp. (submitted), 2010.
- [7] Irsigler, M., Riedl, B., Pany, T., Wolf, R., and Heinrichs, G., "NavX-NCS - A Multi-Constellation RF Simulator: Latest Product Developments and Test Applications," *Proc. ION-GNSS 2009*, Savannah, 2009.
- [8] S.M. Kay. *Fundamentals of Statistical Signal Processing: Detection Theory*, Englewood Cliffs: Prentice Hall, 1998.
- [9] Mattos, G., "High sensitivity GNSS techniques to allow indoor Navigation with GPS and with Galileo," *Proc. ENC-GNSS 2003*, Graz, 2003.
- [10] T. Pany. *Navigation Signal Processing for GNSS Software Receivers*, Norwood: Artech House, 2010.
- [11] Pany T., Riedl, B., Winkel, J., Wörz, T., Schweikert, R., Niedermeier, H., Lagrasta, S., Lopez-Risueno, G., and Jimenez-Banos, D., Coherent Integration Time: The Longer, the Better *InsideGNSS*, vol. 4, no. 6, pp. 52-61, 2009.
- [12] Psiaki, M. L., "Block Acquisition of Weak GPS Signals in a Software Receiver," *Proc. ION-GPS 2001*, Salt Lake City, pp. 2838-2850, 2001.
- [13] Riedl, B., Pany, T., and Winkel, J., "Efficient GNSS Signal Acquisition with Massive Parallel Algorithms using OpenCL on GPUs," *Proc. ION-GNSS 2010*, Portland, pp. (submitted), 2010.
- [14] Sagiraju, P. K., Agaian, S., and Akopian, D., Reduced complexity acquisition of GPS signals for software embedded applications *IEE Proc. Radar, Sonar, and Navigation*, vol. 153, pp. 69-78, 2006.
- [15] Schmid, A. and Neubauer, A., "Performance Evaluation of Differential Correlation for Single Shot Measurement Positioning," *Proc. ION-GNSS 2004*, Long Beach, pp. 1998-2009, 2004.
- [16] Sıçramaz Ayaz, A., Bauernfeind, R., Jang, J. G., Krämer, I., Pany, T., and Eissfeller, B., "Performance Evaluation of Single Antenna Interference Suppression Techniques on Galileo Signals using Real-time GNSS Software Receiver," *Proc. ION-GNSS 2010*, Portland, pp. (submitted), 2010.
- [17] Ward, P. W., "Design Technique for Precise GNSS Receiver Post-Correlation Noise Floor Measurements With Usage Design Examples by the Search and Tracking Processes," *Proc. ION-ITM 2010*, San Diego, 2010.
- [18] E. Göhler, R. Schnieder, J. Winkel, E. Löhnert, "On the development of a high-sensitive GPS/Galileo GNSS ASIC" *Proc. ION-GNSS 2010*, Portland, pp. (submitted), 2010